

Active Damping of a DC Network with a Constant Power Load: An Adaptive Passivity-based Control Approach^{**}

Juan E. Machado^{*} José Arocas-Pérez^{**} Wei He^{***}
Romeo Ortega^{*} Robert Griño^{**}

^{*} *Laboratoire des Signaux et Systèmes, CNRS-Supélec, Plateau du Moulon, 91192, France (e-mail: juan.machado@l2s.centralesupelec.fr, romeo.ortega@lss.supelec.fr).*

^{**} *Institute of Industrial and Control Engineering (IOC), Universitat Politècnica de Catalunya, 08028 Barcelona, Spain (e-mail: jose.arocas@upc.edu, roberto.grino@upc.edu).*

^{***} *Key Laboratory of Measurements and Control of Complex Systems of Engineering, Ministry of Education, School of Automation, Southeast University, 210096 Nanjing, China (e-mail: hwei@seu.edu.cn)*

Abstract: This paper proposes a nonlinear, adaptive controller to increase the stability margin of a direct-current (DC) small-scale electrical network containing a constant power load, whose value is unknown. Due to their negative incremental impedance, constant power loads are known to reduce the effective damping of a network, leading to voltage oscillations and even to network collapse. To tackle this problem, we consider the incorporation of a controlled DC-DC power converter between the feeder and the constant power load. The design of the control law for the converter is based on the use of standard Passivity-Based Control and Immersion and Invariance theories. The good performance of the controller is evaluated with numerical simulations.

Keywords: Constant power loads, active damping, adaptive control, Lyapunov methods, power converters.

1. INTRODUCTION

This note is concerned with the stability analysis of electrical networks with Constant Power Loads (CPLs). It is well-known that, due to their negative impedance characteristic, CPLs induce voltage oscillations or even network collapse, see (Emadi et al., 2006). The analysis of networks with these type of loads started with the work of (Middlebrook, 1976) and has been an active research problem since then, *e.g.*, (Belkhatay et al., 1995b), (Belkhatay et al., 1995a) and (Emadi et al., 2006). We refer the reader to (Singh et al., 2017) and the references therein for a recent review on this topic.

The stability analysis of networks with CPLs has been carried out using different approaches. Linearization methods were used in (Anand and Fernandes, 2013), (Barabanov et al., 2016), and (Marx et al., 2012), see also

(Arocas-Pérez and Griño, 2017). Nonlinear techniques such as the Brayton-Moser mixed potential theory, introduced in (Brayton and Moser, 1964), has been used in (Belkhatay et al., 1995b) and (Cavanagh et al., 2018) to derive sufficient conditions for stability. The use of this technique, to estimate regions of attraction, is reviewed in (Marx et al., 2012). More recently, in (Monshizadeh et al., 2018), using the framework of port-Hamiltonian (pH) systems, see (van der Schaft, 2017), sufficient conditions for stability are presented. It is shown that by imposing upper bounds on the CPLs maximum power, the stability analysis can be concluded using the shifted Hamiltonian as a candidate Lyapunov function. This approach was firstly explored in (Jayawardhana et al., 2007) for general nonlinear systems.

Various controller design techniques have been proposed to enlarge the domain of attraction of this kind of networks with CPLs—a review may be found in (Singh et al., 2017). These stabilization techniques can be divided into passive and active *damping* methods. The former is based on open-loop hardware modifications, whereas the latter implies the modification of existing or added control loops, which may imply the interconnection of additional hardware. In this note we follow the ideas presented in (Carmeli et al., 2012) and (Zhang et al., 2013). In these works, a connection of a *controlled* power

^{*} The work of Juan E. Machado was financially supported by the *National Council of Science and Technology* (CONACyT for its acronym in Spanish) from Mexico. The work of José Arocas-Pérez and Robert Griño was partially supported by the Government of Spain through the *Agencia Estatal de Investigación* Project DPI2017-85404-P and by the *Generalitat de Catalunya* through the Project 2017 SGR 872.

^{**}An abridged version of this paper has been submitted to Congreso Nacional de Control Automático 2018, 10–12 October 2018, San Luis Potosí, México.

converter, in parallel with the CPL (shunt damper), is proposed to increase the stability margins of a small-scale DC network. In (Carmeli et al., 2012), assuming a simplified model for the converter, idealized as a controlled current source, a linear control law is designed. In (Zhang et al., 2013), a full model for the power converter is used. Nonetheless, their stabilization result is based on linearization. A large signal stability analysis, but using approximate techniques, such as the Takagi-Sugeno fuzzy model, is carried out in (Kim et al., 2016).

The main contribution of the present note is to propose a physically realizable nonlinear control law that renders a small-scale DC network, containing a CPL, stable for a wide range of power consumption values from this load. The construction of the controller relies on the use of standard Passivity-Based Control (s-PBC) theory (Ortega et al., 2013). Additionally, using Immersion and Invariance (I&I) theory (Astolfi et al., 2007) the controller is made *adaptive* by including an estimator of the power consumed by the CPL, which is generally *unknown* in a practical context. The good performance of the proposed adaptive controller is evaluated with realistic numerical simulations.

The rest of the paper is structured as follows. In Section 2 we give the model of a small-scale network containing a CPL, analyze its equilibria and describe the stability problem addressed in the paper. The proposed controller configuration, adopted from (Carmeli et al., 2012) and (Zhang et al., 2013), is presented in Section 3. Our main stabilization results are included in Section 4. In Section 5 we present the numerical implementation of our theoretical developments. The note is finalized in Section 6 with a number of concluding remarks and open problems that can be addressed to extend our results.

2. PROBLEM FORMULATION

2.1 Description of the open-loop system

We study a simplified model of a DC power system as shown in Fig. 1. This simple model has been used in the literature, *e.g.*, in (Zhang et al., 2013), (Mosskull, 2015) and (Wu and Lu, 2015), to study the stability problems associated with CPLs. It consists of a DC voltage source supplying electric energy to an instantaneous CPL. The transmission line is simply represented by a lossy inductor and the CPL is connected through a bus capacitor. The dynamic model for this network is given by

$$\begin{aligned} L_1 \dot{i}_1 &= -r_1 i_1 - v_1 + E, \\ C_1 \dot{v}_1 &= i_1 - \frac{P}{v_1}, \end{aligned} \quad (1)$$

where i_1 and v_1 denote the current of the inductor $L_1 > 0$ and the voltage of the capacitor $C_1 > 0$, respectively. The *constant* parameter P corresponds to the power extracted or injected into the network by the CPL, being positive in the former case and negative in the latter. In the sequel, we focus our attention in the critical case $P \geq 0$.

The state space for this system is defined as follows

$$\mathcal{X}_1 := \{(i_1, v_1) \in \mathbb{R}^2 : v_1 > 0\}.$$

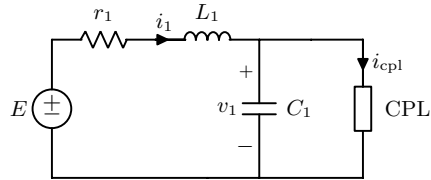


Fig. 1. A DC source supplying power to an instantaneous CPL.

2.2 Equilibrium analysis of the open-loop system

The following proposition pertains to the existence of steady states for the system (1) whose proof, being straightforward, is omitted for brevity.

Proposition 1. The system (1) admits two equilibrium points, which are given by

$$\bar{i}_1 = \frac{E \mp \sqrt{\Delta}}{2r_1}, \quad \bar{v}_1 = \frac{E \pm \sqrt{\Delta}}{2}, \quad (2)$$

Furthermore, these equilibrium points are real if and only if

$$\Delta := E^2 - 4Pr_1 \geq 0 \Leftrightarrow P \leq \frac{E^2}{4r_1}. \quad (3)$$

Remark 2. The system has two equilibria. However, we are mainly interested in operating the system in the equilibrium with the highest value for the voltage \bar{v}_1 and the lowest value for the current \bar{i}_1 . In the sequel, whenever we write (\bar{i}_1, \bar{v}_1) , we are making reference to this particular equilibrium point. In the next section, a controller is added to the system and the control objectives are defined, we will propose a desired value for \bar{v}_1 to be stabilized.

In the next proposition we give sufficient and necessary conditions for the equilibrium point (\bar{i}_1, \bar{v}_1) to be stable. This result follows directly from studying the eigenvalues of the system (1) at (\bar{i}_1, \bar{v}_1) .

Proposition 3. For the system (1), assume that $C_1 < \frac{L_1}{r_1^2}$, then, a necessary condition for (\bar{i}_1, \bar{v}_1) to be stable is given by

$$P \leq \frac{E^2 C_1 L_1 r_1}{(L_1 + C_1 r_1^2)^2}. \quad (4)$$

Furthermore, if this inequality holds strictly, then, (\bar{i}_1, \bar{v}_1) is also asymptotically stable. Lastly, in the case that $C_1 \geq \frac{L_1}{r_1^2}$, the condition

$$P \leq \frac{E^2}{4r_1},$$

is necessary and sufficient for (\bar{i}_1, \bar{v}_1) to be stable.

2.3 Control objectives

To streamline the presentation of our control objectives we make the following observations.

- (i) As seen in (2) and (3), the equilibrium points depend on the value of the parameter P . In particular, the value of \bar{v}_1 decreases when P increases.
- (ii) Proposition 3 shows that, when the capacitance C_1 is not big enough, then, to maintain stability, the power

extraction from the CPL must be strictly smaller than the upper bound for existence of equilibria given in (3).

In the light of these remarks our control objectives are specified as follows.

- CO1 Stabilize the voltage v_1 around a desired value.
- CO2 Relax the upper bound for P established in (4).
- CO3 Achieve these objectives without the knowledge of P .

Condition (b) of Proposition 3 suggests a passive method to achieve these objectives, which consists in increasing the effective capacitance C_1 . This can be done with the connection in parallel of a suitable capacitor and the CPL. Some disadvantages of this approach are mentioned in (Carmeli et al., 2012, Section III.A). Instead of this passive approach, we propose to add a *switched capacitor*. More precisely, following (Carmeli et al., 2012) and (Zhang et al., 2013), we add a shunt damper, that is a power converter in parallel with the CPL. The derivation of the control law for this converter, that ensures the control objectives above, is the main contribution of the paper.

3. AUGMENTED CIRCUIT MODEL

As proposed in (Carmeli et al., 2012) and (Zhang et al., 2013), we consider the addition of a controlled shunt damper between the feeder and the load, as shown in Fig. 2. The damper consists of a DC-DC power converter, composed of two complementary switches u and $(1 - u)$, a lossy inductor L_2 and a capacitor C_2 . The losses associated with the switching devices are modeled with the resistor r_3 .

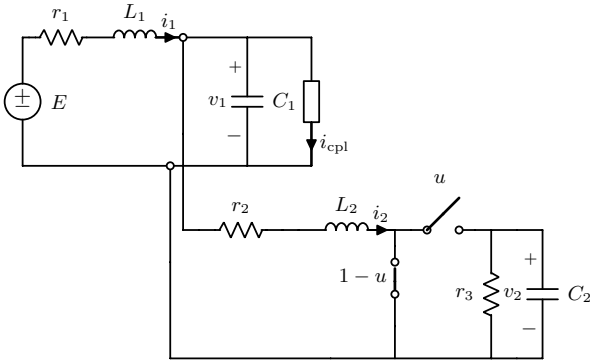


Fig. 2. A shunt damper connected between the feeder and the load for the network of Fig. 1. For the switches, “1” means closed and “0” means open.

The averaged dynamic model of the interconnected system shown in Fig. 2 is given by

$$\begin{aligned}
 L_1 \dot{i}_1 &= -r_1 i_1 - v_1 + E, \\
 C_1 \dot{v}_1 &= i_1 - \frac{P}{v_1} - i_2, \\
 L_2 \dot{i}_2 &= -r_2 i_2 - u v_2 + v_1, \\
 C_2 \dot{v}_2 &= -\left(\frac{1}{r_3}\right) v_2 + u i_2,
 \end{aligned} \tag{5}$$

where i_2 is the current of the inductor $L_2 > 0$, v_2 is the voltage of the capacitor $C_2 > 0$, and the variable $u \in [0, 1]$

represents the duty cycle, which is the control variable for the system.

Before closing this section, and for ease of reference in the sequel, we notice that the system (5) may be written in the classical form $\dot{x} = f(x) + g(x)u$ where

$$x := \text{col}(i_1, v_1, i_2, v_2),$$

is the state vector and

$$f(x) := D^{-1} \begin{bmatrix} -r_1 x_1 - x_1 + E \\ x_1 - \frac{P}{x_2} - x_3 \\ -r_2 x_3 + x_2 \\ -\frac{1}{r_3} x_4 \end{bmatrix}, \quad g(x) := D^{-1} \begin{bmatrix} 0 \\ 0 \\ -x_4 \\ x_3 \end{bmatrix},$$

with $D := \text{diag}\{L_1, C_1, L_2, C_2\}$ and state space

$$\mathcal{X} := \{x \in \mathbb{R}^4 : x_2 > 0, x_4 > 0\}.$$

4. MAIN RESULTS

In this section we propose a nonlinear adaptive controller that ensures that the network under study satisfies the control objectives of Subsection 2.3. Towards this end, we first analyze the set of assignable equilibria and establish constraints on the system parameters for the existence of physically realizable steady states. Second, following s-PBC theory, we design a control law that asymptotically stabilizes a desired equilibrium state assuming the CPL power P is known. Finally, using I&I theory, we present an estimator for P that makes adaptive the proposed controller, preserving the stability property.

4.1 Assignable equilibria

We say that a pair $^1 (\bar{x}, \bar{u}) \in \mathcal{X} \times \mathbb{R}$ is an equilibrium of (5) if and only if

$$f(\bar{x}) + g(\bar{x})\bar{u} = 0. \tag{6}$$

We define the set of *assignable equilibria* \mathcal{E} , as the set of points $\bar{x} \in \mathcal{X}$ for which there exists $\bar{u} \in \mathbb{R}$ such that (6) holds. This set can be computed as follows (see (Ortega et al., 2008, Lemma 2)). Let $g^\perp : \mathcal{X} \rightarrow \mathbb{R}^{3 \times 4}$ be a full-rank left-annihilator of g , i.e., it satisfies $g^\perp(x)g(x) = 0$ for all $x \in \mathcal{X}$ in its rank. Then, \mathcal{E} is given by

$$\mathcal{E} = \{x \in \mathcal{X} : g^\perp(x)f(x) = 0\}. \tag{7}$$

Furthermore, the associated unique equilibrium input \bar{u} is given by

$$\bar{u} = -(g^\top(\bar{x})g(\bar{x}))^{-1} g^\top(\bar{x})f(\bar{x}). \tag{8}$$

In the following proposition we derive the explicit values of $\bar{x} \in \mathcal{E}$ and its associated \bar{u} , which are compatible with the control objectives.

Proposition 4. Fix $\bar{x}_2 > 0$ as a desired operation value for the network. Then, $\bar{x} \in \mathcal{E}$ if and only if

$$P_M(\bar{x}_2) - \frac{\bar{x}_2^2}{r_2} < P < P_M(\bar{x}_2), \tag{9}$$

where

$$P_M(\bar{x}_2) := \frac{\bar{x}_2}{r_1} (E - \bar{x}_2).$$

¹ Following a standard procedure, we let u live in \mathbb{R} even though, being a duty cycle, it is restricted to the set $[0, 1]$. This issue is partially addressed in Corollary 5.

In that case, we can parametrize the remaining equilibrium components as

$$\begin{aligned}\bar{x}_1 &= \frac{E - \bar{x}_2}{r_1}, \\ \bar{x}_3 &= -\frac{Pr_1 - E\bar{x}_2 + \bar{x}_2^2}{r_1\bar{x}_2}, \\ \bar{x}_4 &= \frac{1}{r_1\bar{x}_2} \sqrt{r_3\kappa_1(\bar{x}_2, P)\kappa_2(\bar{x}_2, P)},\end{aligned}\quad (10)$$

where

$$\begin{aligned}\kappa_1(\bar{x}_2, P) &:= -\bar{x}_2^2 + E\bar{x}_2 - r_1P, \\ \kappa_2(\bar{x}_2, P) &:= (r_1 + r_2)\bar{x}_2^2 - r_2E\bar{x}_2 + r_1r_2P.\end{aligned}$$

Furthermore, the associated equilibrium value for the input variable is given by

$$\bar{u} = \sqrt{\frac{\kappa_2(\bar{x}_2, P)}{r_3\kappa_1(\bar{x}_2, P)}}.$$

Proof. The proof follows straightforward if we define

$$g^\perp(x) = \begin{bmatrix} 1 & 0 & 0 & 0 \\ 0 & 1 & 0 & 0 \\ 0 & 0 & x_3 & x_4 \end{bmatrix},$$

and we compute \mathcal{E} and \bar{u} from (7) and (8), respectively. \square

4.2 Equilibrium for maximum power extraction and control realizability

Observe from (9) that the amount of power that can be extracted by the CPL is limited by the choice of \bar{x}_2 . Analogously, the equilibrium value for u , given in (8), depends both on \bar{x}_2 and on P . In the following corollary we choose a desired value of \bar{x}_2 which permits a maximum extraction of power from the CPL. Additionally, we establish conditions on P which guarantee that \bar{u} is strictly smaller than one, *i.e.*, physically realizable with the power converter. The proof of the corollary, being straightforward, is omitted for brevity.

Corollary 5. The largest admissible extracted power $P_M(\bar{x}_2)$ and the constant vectors

$$\bar{x}_2 = \frac{E}{2}. \quad (11)$$

Given this value, $\bar{x} \in \mathcal{E}$ if and only if the extracted power satisfies

$$\frac{E^2(r_2 - r_1)}{4r_1r_2} < P < \frac{E^2}{4r_1}.$$

Furthermore, the associated equilibrium value for u , given by

$$\bar{u} = \sqrt{\frac{E^2(r_1 - r_2) + 4Pr_1r_2}{r_3(E^2 - 4Pr_1)}},$$

is *strictly smaller than one* if and only if the upper-bound on P is restricted even further to

$$P < \frac{E^2(r_2 + r_3 - r_1)}{4r_1(r_2 + r_3)}. \quad (12)$$

4.3 Design of a stabilizing control law

In this subsection we present a control law that renders the desired equilibrium point (10), with \bar{x}_2 given in (11), asymptotically stable. The controller design is carried out following the s-PBC methodology.

For a better readability and following the ideas presented in (Cisneros et al., 2013, Section IV), we show, under the assumption that $x_2(t), x_4(t) > 0$ for all t , that there exists a suitable change of variables for u , which allows us to write the system (5) in the cascade form shown in Fig 3.

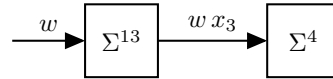


Fig. 3. Block diagram for the cascaded interconnection between the subsystems (13) and (14).

Proposition 6. Define the auxiliary control variable

$$w = x_4u.$$

Then, in the state space \mathcal{X} , the system (5) admits cascade decomposition into the subsystems

$$\Sigma^{13} : \begin{cases} L_1\dot{x}_1 = -r_1x_1 - x_2 + E, \\ C_1\dot{x}_2 = x_1 - \frac{P}{x_2} - x_3, \\ L_2\dot{x}_3 = -r_2x_3 + x_2 - w, \end{cases} \quad (13)$$

and

$$\Sigma^4 : C_2\dot{x}_4 = -\left(\frac{1}{r_3}\right)x_4 + \frac{w}{x_4}x_3. \quad (14)$$

Now, we make the important observation that the system Σ^{13} admits an Euler-Lagrange representation. For more details on the representation of electrical circuits in this formalism, we refer the interested reader to (Ortega et al., 2013).

Proposition 7. Define the vector

$$x^{13} := \text{col}(x_1, x_2, x_3),$$

the matrices

$$\begin{aligned}\mathcal{D} &:= \text{diag}\{L_1, C_1, L_2\} > 0, \\ \mathcal{C} &:= \begin{bmatrix} 0 & 1 & 0 \\ -1 & 0 & 1 \\ 0 & -1 & 0 \end{bmatrix}, \quad R(x^{13}) := \begin{bmatrix} r_1 & 0 & 0 \\ 0 & \frac{P}{x_2^2} & 0 \\ 0 & 0 & r_2 \end{bmatrix},\end{aligned}$$

$$\mathcal{K} := \text{col}(E, 0, 0), \mathcal{G} = \text{col}(0, 0, -1).$$

Then, the system Σ^{13} admits an Euler-Lagrange formulation given by

$$\mathcal{D}\dot{x}^{13} + (\mathcal{C} + R(x^{13}))x^{13} = \mathcal{K} + \mathcal{G}w.$$

The importance of this representation is that it allows a direct application of the s-PBC methodology to define a control law for w which renders the equilibrium point \bar{x}^{13} of Σ^{13} exponentially stable. Consider the following

Proposition 8. For the system Σ^{13} , assign the static state-feedback control

$$w = \phi_2(x^{13}),$$

where

$$\phi_1(x_2) := \bar{x}_1 - \frac{P}{x_2}\bar{x}_2 + k_1(x_2 - \bar{x}_2),$$

$$\phi_2^a := -r_2\phi_1(x_2) - L_2 \left(k_1 + 2\frac{P\bar{x}_2}{x_2^2} \right) f_2(x_1, x_2, x_3),$$

$$\phi_2^b := \bar{x}_2 + k_2(x_3 - \phi_1(x_2)),$$

$$\phi_2(x^{13}) := \phi_2^a + \phi_2^b,$$

and $k_1, k_2 \geq 0$ are arbitrary constants. Then, the equilibrium \bar{x}^{13} is exponentially stable.

Proof. Following an s-PBC methodology, define

$$\hat{x} := (\bar{x}_1, \bar{x}_2, \phi_1(x_2)),$$

and the added damping matrix

$$\mathcal{R}_a := \text{diag}(0, k_1, k_2) \geq 0.$$

Fix $w = \phi_2(x^{13})$. Then, \hat{x} satisfies the expression

$$\mathcal{D}\dot{\hat{x}} + (\mathcal{C} + R(x^{13}))\hat{x} + \mathcal{R}_a(\hat{x} - x^{13}) = \mathcal{K} + \mathcal{G} \cdot \phi_2(x^{13}),$$

Define $e := x^{13} - \hat{x}$. Its derivative satisfies

$$\mathcal{D}\dot{e} + (\mathcal{C} + \mathcal{R}_d(x^{13}))e = 0. \quad (15)$$

where we defined the desired damping matrix

$$\begin{aligned} \mathcal{R}_d(x^{13}) &:= R(x^{13}) + \mathcal{R}_a \\ &= \text{diag}\left\{r_1, \frac{P}{x_2^2} + k_1, r_2 + k_2\right\}, \end{aligned}$$

which is *positive definite* for all $x_2 > 0$. Consider the positive definite function

$$V(e) := \frac{1}{2}e^\top \mathcal{D}e.$$

Its derivative, along solutions of (15), satisfies

$$\dot{V} = -e^\top \mathcal{R}_d(x)e \leq -cV,$$

for a constant $c > 0$, provided $x_2 > 0$. From the last inequality we immediately conclude that the origin of (15) is exponentially stable (Khalil, 2002, Theorem 4.10). Using the fact that $\phi_1(\bar{x}_2) = \bar{x}_3$ we conclude that \bar{x}^{13} is an exponentially stable equilibrium point of Σ^{13} . \square

The next step in our stabilization result, is to show that, when $w = \phi_2(x^{13})$, then x_4 , solutions of the subsystem Σ^4 , converge exponentially to \bar{x}_4 .

Proposition 9. Let $x^{13}(t)$ be any solution of the subsystem Σ^{13} in closed-loop with state-feedback $w = \phi_2(x^{13})$. Then, every solution $x_4(t)$ of Σ^4 , converges exponentially to \bar{x}_4 .

Proof. Consider the change of coordinates

$$z = \frac{1}{2}C_2x_4^2.$$

Then,

$$\dot{z} = -\frac{2}{r_3C_2}z + \phi_2(x^{13})x_3. \quad (16)$$

From Prop. 8, we have that \bar{x}^{13} is an exponentially stable equilibrium point of Σ^{13} . This implies that the term $\phi_2(x^{13})x_3$ remains bounded and converges, exponentially, to the value

$$\begin{aligned} \phi_2(\bar{x}^{13})\bar{x}_3 &= (-r_2\bar{x}_3 + \bar{x}_2)\bar{x}_3 \\ &= (\bar{u}\bar{x}_4)\bar{x}_3, \end{aligned}$$

where we have used the steady state expression

$$-r_2\bar{x}_3 - \bar{u}\bar{x}_4 + \bar{x}_2 = 0.$$

It follows trivially from (16) that

$$z \rightarrow \frac{r_3C_2}{2}\phi_2(\bar{x}^{13})\bar{x}_3 = \frac{r_3C_2}{2}\bar{u}\bar{x}_4\bar{x}_3.$$

exponentially. Using the steady state expression

$$\bar{u}\bar{x}_3 - \frac{1}{r_3}\bar{x}_4 = 0,$$

and restricting $x_4 > 0$, we conclude that $x_4 \rightarrow \bar{x}_4$ exponentially. \square

As a direct application of Props. 8 and 9, we obtain our main result.

Proposition 10. Consider the system (5) in closed-loop with the static state-feedback control

$$u = \gamma(x), \quad (17)$$

where

$$\gamma(x) = \frac{1}{x_4}\phi_2(x_1, x_2, x_3). \quad (18)$$

Then, $\bar{x} \in \mathcal{E}$ is a locally, exponentially stable equilibrium point of the closed-loop system.

4.4 Stabilization assuming an unknown CPL power

In this section we propose an adaptive version of the previously designed controller. Now, we assume that the CPL power P is constant but *unknown*. First, following an I&I technique, a dynamic estimate for P , which we denote by $\hat{P}(t)$, is presented. We show that the error between the estimate and the actual value of P converges to zero exponentially fast for any initial condition.

Proposition 11. For the system (5), assume that P is unknown. Define an on-line estimate for P as follows

$$\dot{\hat{P}}(t) = -\frac{1}{2} \cdot k_3 C_1 v_1^2 + P_1(t), \quad (19)$$

$$\dot{P}_1(t) = k_3 v_1 (i_1 - i_2) + \frac{1}{2} k_3^2 C_1 v_1^2 - k_3 P_1, \quad (20)$$

where $k_3 > 0$ is a free parameter. Then, for any initial condition $(\hat{P}(t_0), P_1(t_0))$, we have that $\lim \hat{P}(t) \rightarrow P$ at exponential rate.

Proof. Define the error estimate

$$\tilde{P}(t) = \hat{P}(t) - P, \quad (21)$$

then, along trajectories of (5) it holds that

$$\begin{aligned} \dot{\tilde{P}}(t) &= \dot{\hat{P}}(t) = -k_3 v_1 C_1 \dot{v}_1 + \dot{P}_1(t) \\ &= -k_3 (v_1 i_1 - P - v_1 i_2) + \dot{P}_1(t) \\ &= -k_3 \tilde{P}(t). \end{aligned} \quad (22)$$

This implies that for any initial condition $\tilde{P}(t_0)$, $\tilde{P}(t)$ is given by

$$\tilde{P}(t) = e^{-k_3(t-t_0)}\tilde{P}(t_0).$$

Hence, $\tilde{P}(t)$ converges to zero at exponential rate. \square

Remark 12. The static controller defined in (17) depends on the components \bar{x}_1 , \bar{x}_2 , and \bar{x}_3 of the desired steady state value $\bar{x} \in \mathcal{E}$ (see Proposition 4). In particular, \bar{x}_2 is assumed to be specified exactly. However, \bar{x}_3 depends linearly on the now assumed unknown CPL power P . In the next proposition we show that the controller is able to achieve the stabilization of \bar{x} even when the designed on-line estimate for P is being used.

Proposition 13. Let $k_3 > 0$ be chosen arbitrarily. For the controller (17), define its adaptive version as

$$u = \hat{\gamma}(x) = \gamma(x)|_{P=\hat{P}(t)}, \quad (23)$$

where γ is given in equation (18) and $\hat{P}(t)$ is the online estimate of P , computed from (19). Then, $(x, \hat{P}) = (\bar{x}, P)$, with $\bar{x} \in \mathcal{E}$, is an asymptotically stable equilibrium point of the extended dynamics conformed by (5), (19) and (23).

Proof. First, let us note that there exist suitable continuous mappings $\lambda : x \mapsto \lambda(x)$, $\mu : x \mapsto \mu(x)$, and $\xi : x \mapsto \xi(x)$, not written here for space reasons, such that the control laws γ , defined in (17), can be written as

$$\gamma(x) = \lambda(x)P^2 + \mu(x)P + \xi(x). \quad (24)$$

If we substitute P by its estimate $\hat{P}(t)$ given in (19), which in turn can be written in terms of the error estimate $\tilde{P}(t)$ defined in (21), then we can write an estimate of γ , denoted by $\hat{\gamma}$, as follows

$$\begin{aligned}\hat{\gamma}(x) &= \lambda(x)\hat{P}^2(t) + \mu(x)\hat{P}(t) + \xi(x) \\ &= \lambda(x)\left(P + \tilde{P}(t)\right)^2 + \mu(x)\left(P + \tilde{P}(t)\right) + \xi(x) \\ &= \gamma(x) + \epsilon\left(x, \tilde{P}(t)\right),\end{aligned}\quad (25)$$

where

$$\epsilon\left(x, \tilde{P}(t)\right) = \tilde{P}(t)\left[\lambda(x)\left(2P + \tilde{P}(t)\right) + \mu(x)\right].$$

Notice that we recover the controller (24), which assumes an exact knowledge of P , plus a vanishing term. Now, we explore the stability of the overall system conformed by (5), (22) and (25). Let $\bar{x} \in \mathcal{E}$ a desired equilibrium point to be stabilized. Using $u = \hat{\gamma}(x)$ as a control law, the system (5) adopts the form

$$\begin{aligned}\dot{x} &= f(x) + g(x) \cdot \hat{\gamma}(x) \\ &= f(x) + g(x) \cdot \left(\gamma(x) + \epsilon\left(x, \tilde{P}(t)\right)\right) \\ &= f(x) + g(x) \cdot \gamma(x) + g(x) \cdot \epsilon\left(x, \tilde{P}(t)\right).\end{aligned}\quad (26)$$

Observe that this system is in cascade with (22). Furthermore, if $\tilde{P}(t)$ is assumed to be zero, then \bar{x} is an asymptotically stable equilibrium point, see Proposition 10. Recalling that $\tilde{P} = 0$ is an exponentially stable equilibrium point for (22), we use (Sepulchre et al., 2012, Proposition 4.1), to conclude that $(x, \tilde{P}) = (\bar{x}, 0)$ is an asymptotically equilibrium point of the cascaded system conformed by (22) and (26). \square

5. NUMERICAL VALIDATION

In this section, we numerically evaluate the performance of the proposed adaptive controller. The system physical parameters are taken according to Table 1, and the parameters for the adaptive controller, presented in equation (23), are taken as

$$k_1 = 30, \quad k_2 = 0.78, \quad k_3 = 1000.$$

Simulations for the closed-loop system (5) and (23) were done taking the initial condition

$$x(0) = \text{col}(40, 12, 31.6667, 612.3611),$$

which corresponds to the equilibrium point $\bar{x}|_{P=100}$, with the particular value of \bar{x}_2 proposed in equation (11), given by

$$\bar{x}_2 = \frac{1}{2}E = 12 \text{ V},$$

see Prop. 4. Then, at $t = 1 \mu\text{s}$, a step change in the CPL power, from $P = 100 \text{ W}$ to $P = 479 \text{ W}$ is introduced. The control objective is to stabilize the *new* equilibrium point

$$\bar{x}|_{P=479} = \text{col}(40, 12, 0.0833, 31.6222) \in \mathcal{E}.$$

We point out that the controller is able to keep the same desired value for \bar{x}_2 regardless of the change in the value of P . Nonetheless, the rest of the coordinates of \bar{x} change, see equation (10). For clarity we use a logarithmic scale for the time to better appreciate the transient response of the system.

Fig. 4 shows the plot of $x_2(t)$. Clearly, the controller is able to maintain the value of x_2 around the desired value

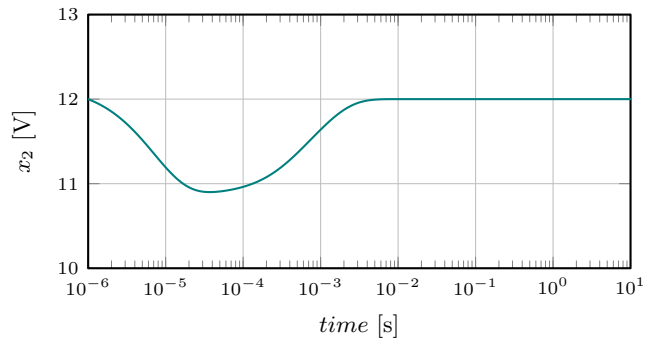


Fig. 4. Plot of $x_2(t)$ for the system (5) using the adaptive controller of equation (23). At $t = 1 \mu\text{s}$ a step change from $P = 100 \text{ W}$ to $P = 479 \text{ W}$ is introduced.

of $\bar{x}_2 = \frac{1}{2}E$, in spite of the change in the power consumed by the CPL.

Fig. 6 shows the plot of $u(t)$. Observe that its value is always bounded within zero and one. Hence, the controller is physically realizable with the proposed DC-DC power converter.

We underscore that the new CPL power satisfies the upper bound for stability established in (12), which with our numerical parameters reads as

$$P < 479.85 \text{ W}.$$

This condition clearly relaxes the *necessary* condition for stability presented in Proposition 3, which says that if the CPL power satisfies

$$P > \frac{E^2 C_1 L_1 r_1}{(L_1 + C_1 r_1^2)^2} = 276.9 \text{ W},$$

then, the network *without* the shunt damper is unstable. Observe that the new CPL power value is very close to the maximum admissible value for existence of equilibria written in (3), which in our case corresponds to $P \leq 480 \text{ W}$. Hence, the addition of the shunt damper, operating under our adaptive controller, achieves the stabilization of a desired equilibrium point $\bar{x} \in \mathcal{E}$ for a wide range of values for the CPL. For the sake of completeness, in Fig. 5, we present the plots of the state variables $x_1(t)$, $x_3(t)$, $x_4(t)$ and the estimated power against the time..

In Fig. 7 we present the plot of $x_2(t)$ for two scenarios: with the shunt damper and without it. This results were obtained by repeating the previous simulation but now taking the final value of P as $P = 260 \text{ W}$ at $t = 1 \text{ ms}$. For network without the shunt damper, the steady state voltage \bar{x}_2 clearly decreases with the increase in the value of the CPL power. Additionally, an oscillatory behavior is present during the transient. Lastly, when the shunt damper is connected, the stabilization of x_2 around a desired value is achieved, independently of the CPL consumption.

Table 1. Parameters for the circuit in Fig. 2

$r_1 = 0.3 \Omega$	$L_1 = 85.0 \mu\text{H}$	$C_1 = 200 \mu\text{F}$	$E = 24.0 \text{ V}$
$r_2 = 5 \text{ m}\Omega$	$L_2 = 100 \mu\text{H}$	$C_2 = 1.0 \text{ mF}$	$r_3 = 1 \text{ k}\Omega$

Remark 14. In the simulations, we have focused on the stabilization of \bar{x} with a fixed \bar{x}_2 as proposed in Corollary 5. However, other values for \bar{x}_2 can be chosen as long

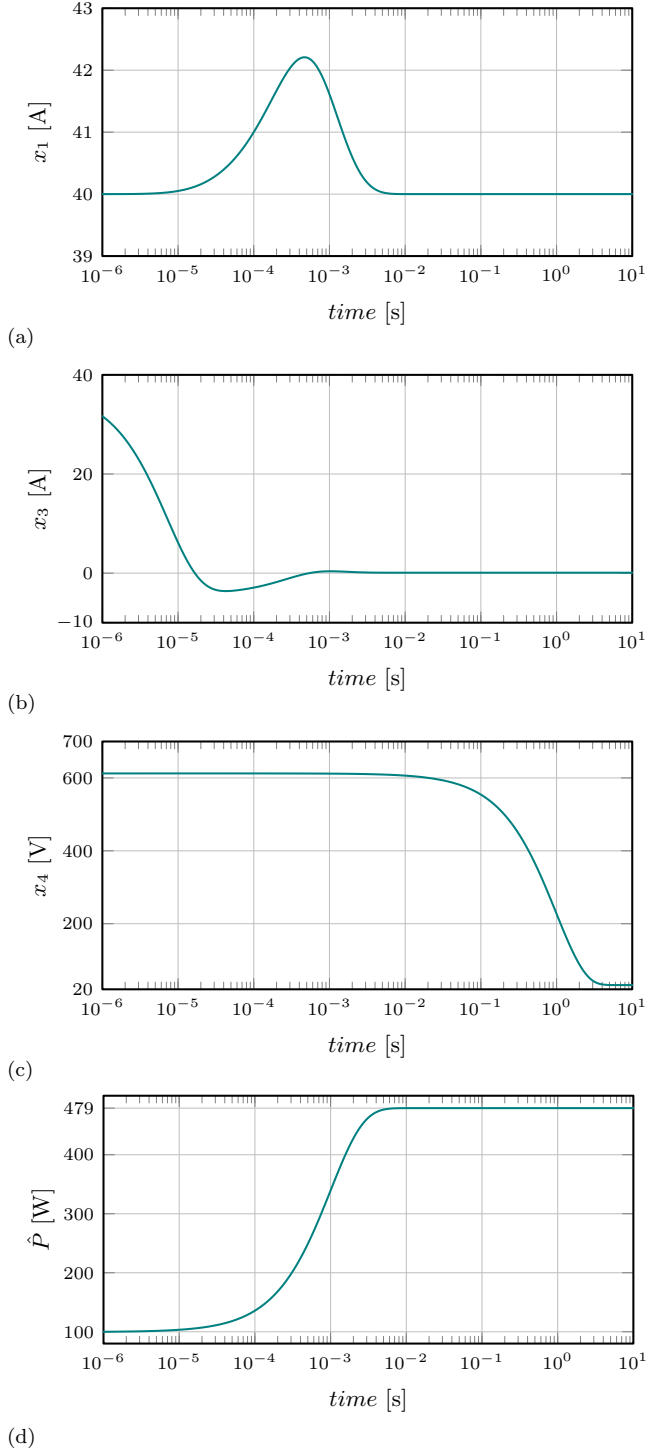


Fig. 5. Plot of (a) $x_1(t)$, (b) $x_3(t)$, (c) $x_4(t)$ and (d) $\hat{P}(t)$ for the system (5) using the adaptive controller of equation (23). At $t = 1 \mu\text{s}$ a step change from $P = 100 \text{ W}$ to $P = 479 \text{ W}$ is introduced.

as inequalities (9) are satisfied. Diverse numerical experiments showed a dependency between the chosen value of \bar{x}_2 and the energetic efficiency of the power converter. Further analysis of this phenomenon is left as a future research.

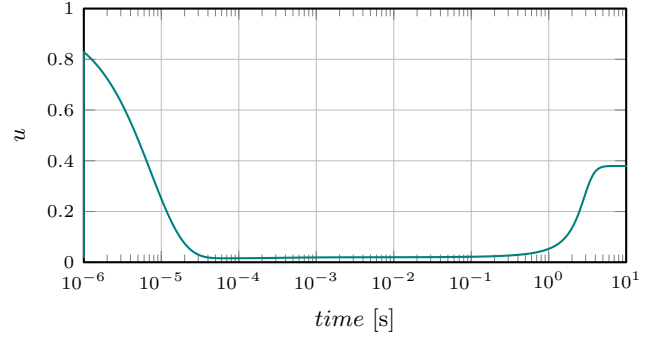


Fig. 6. Plot of $u(t)$ for the system (5) using the adaptive controller of equation (23). At $t = 1 \mu\text{s}$ a step change from $P = 100 \text{ W}$ to $P = 479 \text{ W}$ is introduced.

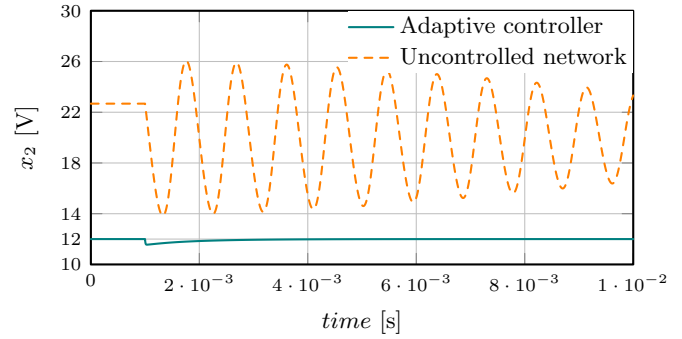


Fig. 7. Plot of $x_2(t)$ with and without the shunt damper. At $t = 1 \text{ ms}$ a step change from $P = 100 \text{ W}$ to $P = 260 \text{ W}$ is introduced.

6. CONCLUSIONS AND FUTURE WORK

In this paper we have proposed a nonlinear stabilization method for a DC small-scale power system supplying electric energy to a CPL. This is done by incorporating an active shunt damper, consisting of a controlled DC-DC power converter connected at the point of common coupling, exactly between the feeder and the load. Using s-PBC and I&I theories, a nonlinear adaptive control law for the shunt damper is designed. It permits the stable operation of the network for a wide range of values of the CPL and is able to relax some necessary stability bounds that are imposed when the system operates *without* the shunt damper. Through realistic numerical simulations, we have illustrated the satisfactory behavior of the designed controller.

The results of this paper can be extended in the following directions:

- Explicitly compute estimates for the Region of Attraction of the system in closed-loop. Particularly, for the case when the power estimate, designed in Section 4.4, is used.
- Theoretically evaluate the robustness, against parameter uncertainty, of the proposed adaptive control.
- Design an observer for the variable x_1 , which is, in some practical scenarios, difficult to measure. We underscore that both, our controller and our power estimator, explicitly depend on this value.

-Further investigate the dependency between the chosen value \bar{x}_2 and the energetic efficiency of the power converter, see Remark 14.

- Analyze the viability of applying the present stabilization result to the case of multi-port networks with a distributed array of CPLs.

REFERENCES

- Anand, S. and Fernandes, B.G. (2013). Reduced-order model and stability analysis of low-voltage DC microgrid. *IEEE Transactions on Industrial Electronics*, 60(11), 5040–5049.
- Arocas-Pérez, J. and Griño, R. (2017). A local stability condition for dc grids with constant power loads. *IFAC-PapersOnLine*, 50(1), 7–12.
- Astolfi, A., Karagiannis, D., and Ortega, R. (2007). *Non-linear and adaptive control with applications*. Springer Science & Business Media.
- Barabanov, N., Ortega, R., Griño, R., and Polyak, B. (2016). On existence and stability of equilibria of linear time-invariant systems with constant power loads. *IEEE Transactions on Circuits and Systems I: Regular Papers*, 63(1), 114–121.
- Belkhat, M., Cooley, R., and Abed, E. (1995a). Stability and dynamics of power systems with regulated converters. In *IEEE Proceedings of ISCAS'95 - International Symposium on Circuits and Systems*, 143–145. Seattle, United States of America.
- Belkhat, M., Cooley, R., and Witulski, A. (1995b). Large signal stability criteria for distributed systems with constant power loads. In *IEEE Proceedings of the Power Electronics Specialist Conference (PESC'95)*, 1333–1338. Atlanta, United States of America.
- Brayton, R.K. and Moser, J.K. (1964). A theory of nonlinear networks – i. *Quarterly of Applied Mathematics*, 22(1), 1–33.
- Carmeli, M.S., Forlani, D., Grillo, S., Pinetti, R., Ragaini, E., and Tironi, E. (2012). A stabilization method for dc networks with constant-power loads. In *IEEE International Energy Conference and Exhibition (ENERGYCON)*, 617–622. Florence, Italy.
- Cavanagh, K., Belk, J.A., and Turitsyn, K. (2018). Transient stability guarantees for ad hoc dc microgrids. *IEEE Control Systems Letters*, 2(1), 139–144.
- Cisneros, R., Mancilla-David, F., and Ortega, R. (2013). Passivity-based control of a grid-connected small-scale windmill with limited control authority. *IEEE Journal of Emerging and Selected Topics in Power Electronics*, 1(4), 247–259.
- Emadi, A., Khaligh, A., Rivetta, C.H., and Williamson, G.A. (2006). Constant power loads and negative impedance instability in automotive systems: definition, modeling, stability, and control of power electronic converters and motor drives. *IEEE Transactions on Vehicular Technology*, 55(4), 1112–1125.
- Jayawardhana, B., Ortega, R., García-Canseco, E., and Castaños, F. (2007). Passivity of nonlinear incremental systems: Application to PI stabilization of nonlinear RLC circuits. *Systems & Control Letters*, 56(9), 618–622.
- Khalil, H.K. (2002). *Nonlinear Systems*. Prentice Hall, 3rd edition.
- Kim, H.J., Kang, S.W., Seo, G.S., Jang, P., and Cho, B.H. (2016). Large-signal stability analysis of dc power system with shunt active damper. *IEEE Transactions on Industrial Electronics*, 63(10), 6270–6280.
- Marx, D., Magne, P., Nahid-Mobarakeh, B., Pierfederici, S., and Davat, B. (2012). Large signal stability analysis tools in dc power systems with constant power loads and variable power loads: a review. *IEEE Transactions on Power Electronics*, 27(4), 1773–1787.
- Middlebrook, R.D. (1976). Input filter considerations in design and application of switching regulators. *IEEE Industry Applications Society Annual Meeting*, 366–382.
- Monshizadeh, P., Machado, J.E., Ortega, R., and van der Schaft, A. (2018). Power-controlled hamiltonian systems: Application to electrical systems with constant power loads. *CoRR*, abs/1802.02483.
- Mosskull, H. (2015). Optimal dc-link stabilization design. *IEEE Transactions on Industrial Electronics*, 62(8), 5031–5044.
- Ortega, R., van der Schaft, A., Castanos, F., and Astolfi, A. (2008). Control by interconnection and standard passivity-based control of port-hamiltonian systems. *IEEE Transactions on Automatic Control*, 53(11), 2527–2542.
- Ortega, R., Loria, A., Nicklasson, P.J., and Sira-Ramirez, H.J. (2013). *Passivity-based control of Euler-Lagrange systems: Mechanical, electrical and electromechanical applications*. Springer Science & Business Media.
- Sepulchre, R., Jankovic, M., and Kokotovic, P.V. (2012). *Constructive nonlinear control*. Springer Science & Business Media.
- Singh, S., Gautam, A.R., and Fulwani, D. (2017). Constant power loads and their effects in dc distributed power systems: A review. *Renewable and Sustainable Energy Reviews*, 72, 407–421.
- van der Schaft, A.J. (2017). *L2-Gain and Passivity Techniques in Nonlinear Control*. Springer International Publishing, 3rd edition.
- Wu, M. and Lu, D.D.C. (2015). A novel stabilization method of lc input filter with constant power loads without load performance compromise in dc microgrids. *IEEE Transactions on Industrial Electronics*, 62(7), 4552–4562.
- Zhang, X., Ruan, X., Kim, H., and Chi, K.T. (2013). Adaptive active capacitor converter for improving stability of cascaded dc power supply system. *IEEE Transactions on Power Electronics*, 28(4), 1807–1816.